HIGH TEMPERATURE OXIDATION BEHAVIOR OF ODS IRON-BASE ALLOYS FOR NUCLEAR ENERGY APPLICATION

M. Li, Z. Zhou, L. Liao, W. Chen and C. Ge
School of Materials Science and Engineering, University of Science and Technology Beijing, Beijing 100083, China

Abstract

Oxide dispersion strengthened (ODS) iron based alloys are considered as promising high temperature structural material for advanced nuclear energy systems due to its higher creep strength and radiation damage resistance than conventional commercial steels. In this study, the oxidation behavior of ODS iron based alloys with different Cr content (12-18%) was investigated by exposing samples at high temperature of 700℃ and 1000℃ in atmosphere environment, the exposure time is up to 500 h. Results showed that 14Cr and 18Cr ODS alloys exhibited better oxidation resistance than 12Cr ODS alloys. For the same chromium content, the oxidation resistance of ODS alloys are better than that of non-ODS alloys.

1. Introduction

Ferritic steels have excellent radiation resistance and inferior elevated temperature strength compared to conventional austenitic steels. Oxide dispersion strengthened (ODS) steels produced by powder metallurgical techniques are a class of advanced materials which present good mechanical strength at elevated temperature and high resistance to swelling under heavy radiation[1,2] due to the addition of Y_2O_3 and subsequent mechanical alloying (MA), compared to other conventional heat resistant steels. The better performance suggests these are the promising candidate for structural components in fusion reactors and Generation IV reactors, especially in the supercritical water-cooled reactor (SCWR). However the higher operating temperature leads to more corrosive environment, an assessment of the long-term stability of structural components is required. Since a high Cr content is effective in preventing the corrosion at high temperature, high Cr content ODS ferritic steels are promising for SCWR. But on the other hand, too much Cr addition will lead to the deterioration of the mechanical strength. The addition of Al is often used as a deoxidization material in steel production, and it also improves the Charpy impact property of the high Cr content ODS steels. Relevant studies highlight that the addition of Cr and Al to ODS steels can improve the resistance to corrosion in SCWR [3, 4]. High temperature oxidation behavior is also an impotant property for evaluation ODS steels as candidate materials for fuel cladding and other structural components in nuclear plants.

In this study, different Cr content (12-18%) ODS ferritic alloys were investigated by exposing samples at high temperature to an atmosphere environment. The purpose of this study was to investigate the oxidation behavior and describe the effect of different chromium and aluminum concentration at different temperature on corrosion resistance.

2. Experimental

2.1 Materials

Six mechanical alloyed (MA) ODS alloys were investigated: 12Cr-ODS alloy, 14Cr-ODS alloy, 18Cr-ODS alloy and the corresponding non-ODS alloy (12Cr, 14Cr and 18Cr, designated M1, M3 and M5). The nominal chemical compositions of the alloys are summarized in Table 1. Four wt% Al was presented in the 18Cr alloys. The mixtures of nitrogen atomized powders and 30 nm Y_2O_3 powders were mechanically alloyed via a planetary ball mill and then HIPed. For comparison, the rest of the atomized powders were directly HIPed without addition of Y_2O_3 powers. All the HIPed specimens were machined with dimensions of $8 \times 6 \times 2$ mm^3 and then polished with 3.5 μm diamond polishing slurry. Prior to oxidation, the specimens were ultrasonically cleaned in acetone and methanol.

Table 1 Nominal chemical composition of iron based materials used in this investigation (wt %)

Materials	C	Si	Mn	Cr	V	W	Ta	Ti	Al	Y_2O_3
12Cr (M1)	0.13	0.15	0.5	12	0.18	2	0.08	0.5	-	-
12-ODS (M2)										0.35
14Cr (M3)	0.06	0.2	-	14	-	2	-	0.5	-	-
14Cr-ODS (M4)										0.16
18Cr (M5)	0.02	0.15	-	18	-	2	-	0.5	4	-
18Cr-ODS (M6)										0.35

2.2 Oxidation test

The oxidation tests were performed on a curved surface of quartz glass to maximize the interface with dry air. 12-18Cr specimens were investigated at 700℃, 1000℃ and 1100℃ for various periods. Due to the high resistance to oxidation of the high Cr alloy, 700℃ is too low to observe the oxidation behaviour. Thereby 14Cr and 18Cr alloys were not studied in the investigation at 700℃. 1200℃ and 1300℃ were chosen for the 18Cr alloys. SEM with back-scatter mode and EDS was used for the analysis of the thickness and state of the oxidized scale, and the observation of oxide layers on surface and cross section of the specimens. The elemental distribution was measured by means of electron probe microanalysis (EPMA). In order to analyze the structural change of the corroded surfaces of the specimens, X-ray diffraction (XRD) analysis was performed.

3. Results and discussion

3.1 Oxide microstructure, morphology and compositions

Fig. 1 shows the morphologies of the oxide scales formed on the M1 and M2 surfaces after exposure at 700℃ for up to 500 h. For the M1 surface, the whole of the surface was covered with regular spinel type oxides and the grain size was ~1 μm. However, the spinel type oxides were not found on the surface of the M2 sample. Instead, complex oxides with irregular shapes were covered the surface. Surface analysis via EDS indicated the presence of Fe, Cr, O and Mn as major constituents.

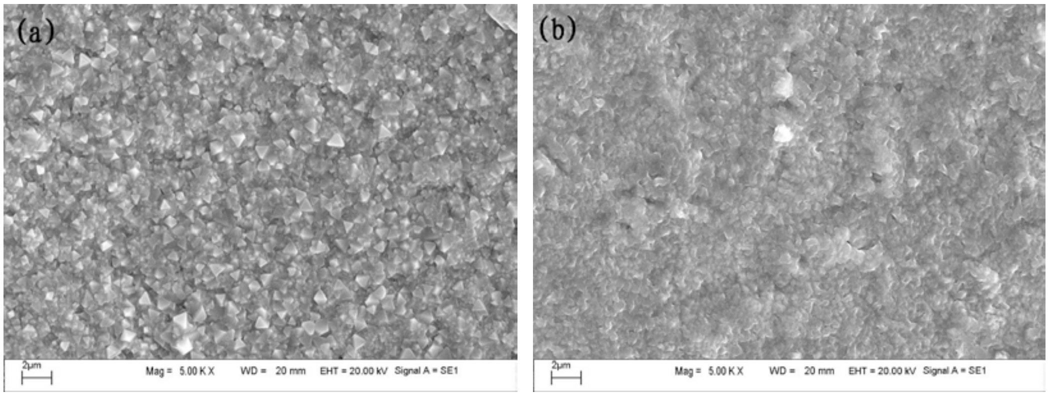

Figure 1 SEM images of the surface morphologies obtained on (a) M1 and (b) M2 after 500 h oxidation at 700□.

XRD analyses were performed and the results were shown in Figure 2. The Fe-Cr solid solution phase with the α-Fe type structure originating from the substrate material was identified in both alloys prior to the oxidation test. Differences appeared after exposure for 500 h at 700□. XRD results, shown in Fig. 2b, revealed that the spinel phase with a composition close to $MnFe_2O_4$, as well as an oxide with $Cr_{1.3}Fe_{0.703}$ were found on the surface of the M1 surface. $MnFe_2O_4$ and Mn_2O_3 were identified on the surface of the M2 sample. The α-Fe phase, with strong intensity, was observed on both specimens, indicating that the oxide scale was very thin. In fact, the oxide scale was too thin to identify by means of SEM. The stronger intensity of $MnFe_2O_4$ for M2 also revealed that the $FeMn_2O_4$ layer was thicker than that for the M1 surface. The regular spinel structural phase could not be observed from the SEM image as shown Figure 1b.

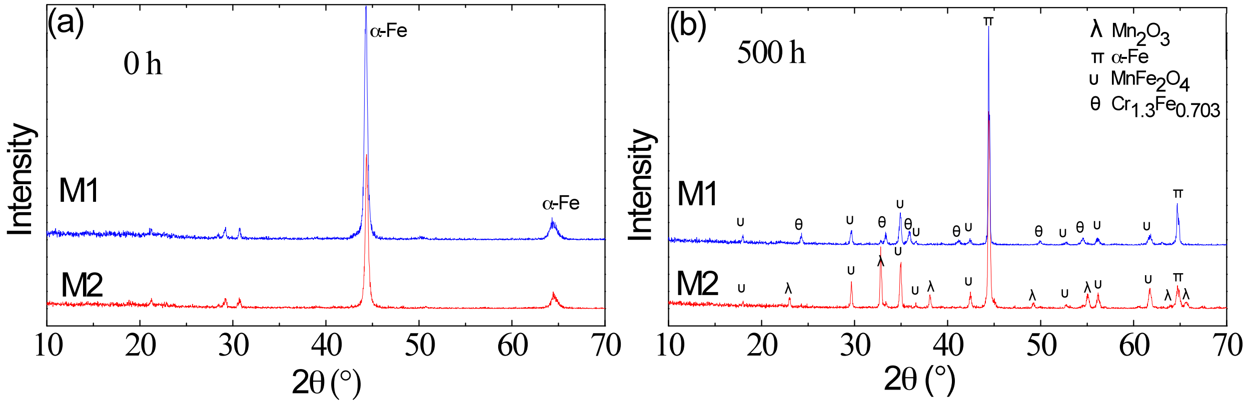

Figure 2 X-ray diffraction patterns obtained from the 12Cr alloys exposed in atmosphere environment at 700 □ for (a) 0 h and (b) 500 h.

EPMA images in linescan mode also showed the differences in the scale composition, as shown in Fig.3. Fig. 3a reveals that the outer layer contained more Cr than other major elements. Mn and O existed in the layer close to the matrix. The results correspond with those shown in Figure 2b, namely, the presence of a minor $Cr_{1.3}Fe_{0.703}$ oxide phase located at the outer surface. Figure 3b shows the distribution of major elements across the oxide scale of the M2 sample. The results indicated that the outer layer contained Mn_2O_3. This may be the reason why the spinel structure disappeared from the surface of the oxide scale, as shown in Fig. 1b: Mn_2O_3 covered the surface of $MnFe_2O_4$. In addition, the change of location of the Cr-rich layer in the oxide scale on the surface of the ODS and non-ODS alloys is an interesting question, and further studies are required.

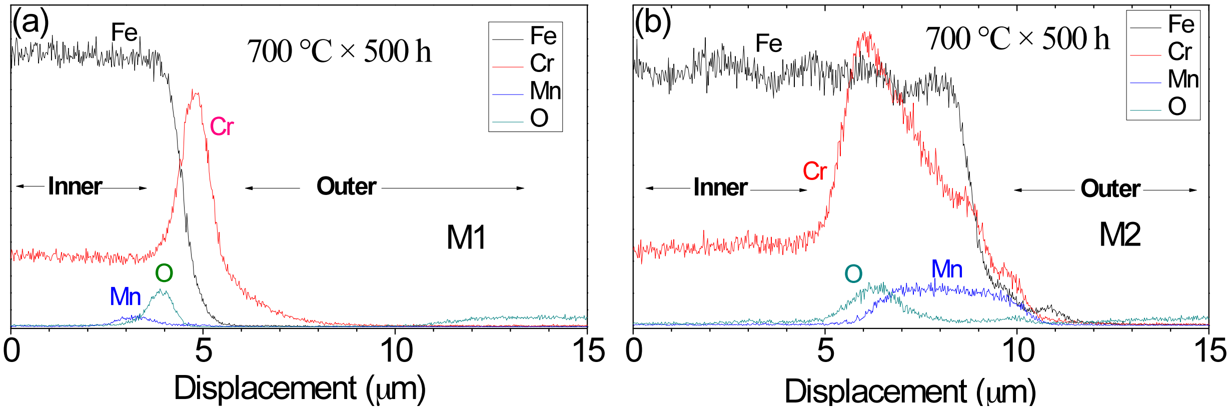

Figure 3 Major elements distribution across the scale thickness using EPMA in linescan mode.

3.2 Evaluation of the resistance to oxidation

Fig. 4 shows the SEM images of the specimen surface after air cooling at 1000□. The M1 sample was exposed for 1 h and then air cooling was performed. The M2 sample was exposed for up to 8 h. The air cooling was performed after 1 h, 2 h, 4 h and 8 h. The specimens were put into the furnace after cooling until the test was finished. The results of air cooling of the M1 sample are shown Fig. 4a. Part of scale spalled off during cooling to room temperature, as shown at the right top corner of Fig. 4a. The SEM image of the M1 sample showed that cracks spread all over the surface and large conglomerations of oxides (~5 μm in size) were observed on the surface. EDS revealed that these large conglomerations contained Fe and O. The M2 sample had excellent resistance to spallation during air cooling, as shown at the right top corner of Fig. 4b. The SEM image showed presence of $MnCr_2O_4$ and $Mn_{1.5}Cr_{1.5}O_4$ spinel phase, and the presence of which was confirmed via EDS and XRD analyses. The surface was covered with 3~10 μm nodules, and no cracks were observed. Uneven surfaces with no spinel type oxide were observed by SEM after oxidation for 500 h at 700□ for the M2 sample, however spinel phases were observed after exposure for 8 h at 1000□. Compared with the M1 sample at 700℃ and 1000℃, the observations indicated a change of oxidation mechanism: Small spinel crystals on the surface, then the crystal grew, following nodules appeared, and finally scales spalled. The results show that the MA-ODS process can effectively retard oxidation.

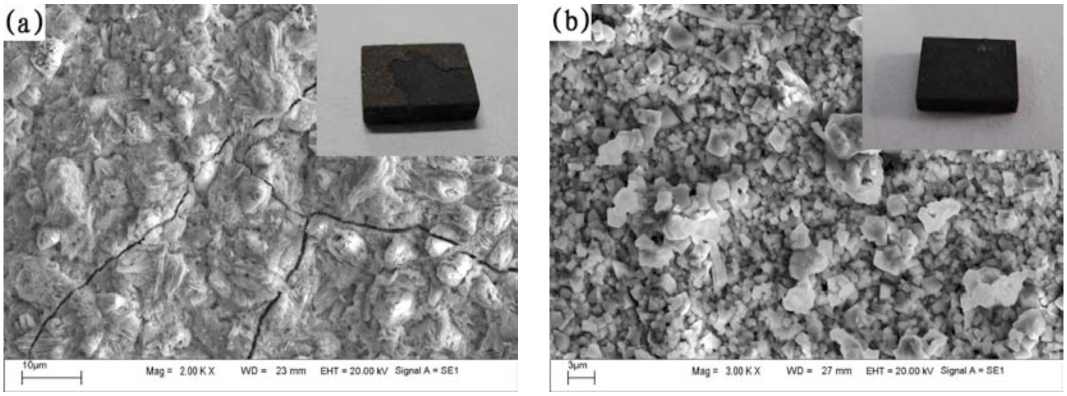

Figure 4 SEM images of 12Cr alloys with (a) holding 1h before a single air cooling for the M1 sample and (b) total 8 and 4 air cooling cycles for the M2 sample at 1000℃.

Fig. 5 shows the surface images of the M3 and M4 samples after exposure for 2 h at 1000℃. Air cooling was conducted after oxidation. Spallation occurred after air cooling for the M3 sample, as shown on the right top corner. The flower-shape ferric oxide observed in Fig. 5a revealed coarsening and rapid growth of oxides at 1000℃. Coarse surface were observed for M4, exhibiting local areas composed of non-uniform oxide grains with nodule-like oxides. No spallation was observed, as shown at the right top corner in Fig. 5b.

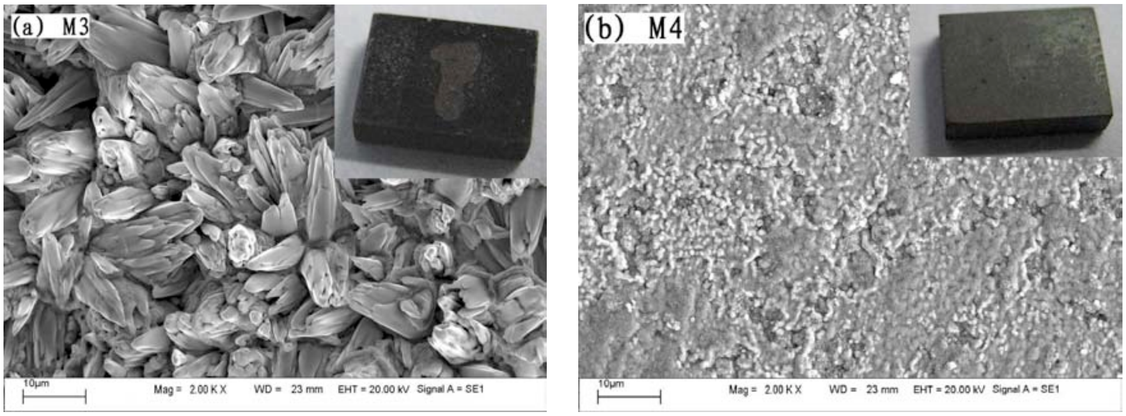

Figure 5 SEM images of 14Cr alloys after exposure in air for 2h at 1000℃.

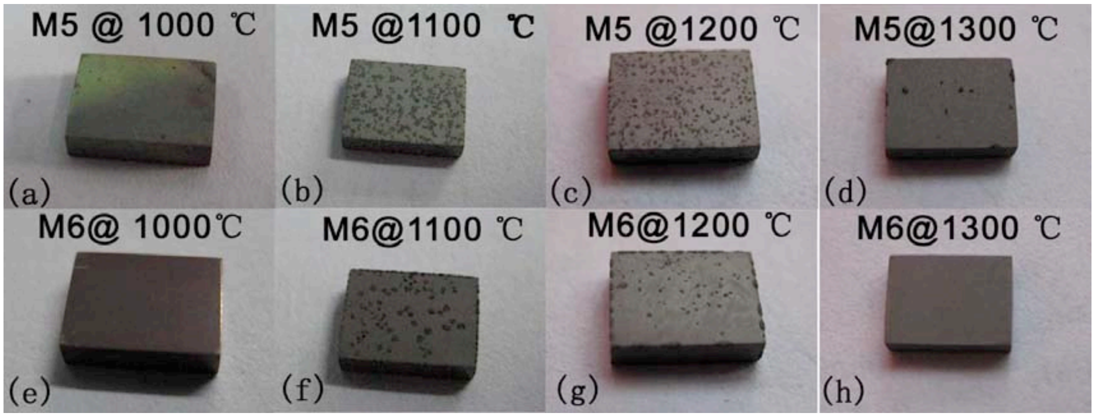

Figure 6 Comparison of specimens tested at various temperatures for 2 h.

In order to suppress the corrosion and improve the mechanical properties, Al was added to the 18Cr alloy. The oxidation test was performed at various temperatures from 1000℃ to 1300℃, and the exposure time in air was 2 h. Fig. 6 compares the specimens at various temperatures. No obvious oxidation occurred at 1000℃ and the two alloys exhibited a metallic luster after oxidation. Nodules covered the surface of both alloys when the temperature increased to 1100℃, and the nodules on the M5 sample were more homogeneous and smaller than that on the M6 surface. EDS revealed that nodules on the M5 sample contained Fe, Cr, Ti, Al and O, and the nodules on the M6 sample contained Fe, Cr, Al and O. No obvious changes in the nodules occurred when temperature increased to 1200℃, whereas the nodules disappeared from the M6 sample and a few nodules were observed on the M5 sample when the temperature increased to 1300℃. EDS indicated an increasing content of alumina, and this indicated alumina played an important role in the oxidation reaction. Generally speaking, the dispersed oxide suppresses the spalling of the alumina film through trapping of the detrimental element S, and the ODS alloys form a diffusion barrier enriched in Y at the alumina film/alloy interface and suppress the penetration of alloying elements into the film, whereas Cr also plays a important role in 18Cr alloys. The competition between Al and Cr in oxidation reaction should be clarified in further studies.

4. Conclusion

Six alloys were investigated by heating in air for various times at different temperatures. The results of this study are summarized as follows:

(1) 12Cr-ODS alloys form a thin oxide scale composed of $MnFe_2O_6$ and Mn_2O_3 and the oxide scale of 12Cr non-ODS alloy contain $MnFe_2O_4$ and a $Cr_{1.3}Fe_{0.703}$ oxide after exposure at 700□ for 500 h.

(2) ODS alloys have excellent resistance to oxide scale spallation in air.

(3) High Cr content alloys exhibit better oxidation resistance.

(4) The addition of Al play an important role in suppressing the oxidation of these steels.

Acknowledgements

This work is supported by the National Basic Research Program of China (973 Program, No. 2007CB209801).

5. References

[1] S. Ukai, S. Ohtsuka, T. Kaito, etal, “High-temperature strength characterization of advanced 9Cr-ODS ferritic steels”, Materials Science and Engineering A, Vol. 510-511, 2009, pp.115-120.

[2] D.T. Hoelzer, J. Bentley, M.A. Sokolov, etal, "Influence of particle dispersions on the high-temperature strength of ferritic alloys", Journal of Nuclear Materials, Vol.367-370, Part 1, 2007, pp.166-172.

[3] H.S. Cho, H. Ohkubo, N. Iwata, etal. "Improvement of compatibility of advanced ferritic steels with super critical pressurized water toward a higher thermally efficient water-cooled blanket system", Fusion Engineering and Design, Vol. 81, Iss. 8-14, 2006, pp.1071-1076.

[4] J. S. Lee, A. Kimura, S. Ukai, etal, "Effects of hydrogen on the mechanical properties of oxide dispersion strengthening steels", Journal of Nuclear Materials, Vol. 329-333,2004, pp.1122-1126.